CHEMISTRY & SUSTAINABILITY

CHEMSUSCHEM

ENERGY & MATERIALS

Accepted Article

Title: Plasma-driven in situ production of hydrogen peroxide for biocatalysis

Authors: Abdulkadir Yayci, Álvaro Gómez Baraibar, Marco Krewing, Elena Fernandez Fueyo, Frank Hollmann, Miguel Alcalde, Robert Kourist, and Julia Elisabeth Bandow

To be cited as: *ChemSusChem* 10.1002/cssc.201903438

Link to VoR: http://dx.doi.org/10.1002/cssc.201903438

A Journal of

ChemPubSoc Europe

WILEY-VCH

www.chemsuschem.org

Plasma-driven *in situ* production of hydrogen peroxide for biocatalysis

Abdulkadir Yayci[a] (ORCID: 0000-0003-4615-8981), Álvaro Gómez Baraibar[b] (ORCID: 0000-0001-7191-7316), Marco Krewing[a] (ORCID: 0000-0002-5315-8755), Elena Fernandez Fueyo[c] (ORCID: 0000-0002-5079-2240), Frank Hollmann[c] (ORCID: 0000-0003-4821-756X), Miguel Alcalde[d] (ORCID: 0000-0001-6780-7616), Robert Kourist[b,e] (ORCID: 0000-0002-2853-3525) and Julia E. Bandow[a]* (ORCID: 0000-0003-4100-8829)

[a] Applied Microbiology, Faculty of Biology and Biotechnology
Ruhr University Bochum
Universitätsstraße 150, 44780 Bochum, Germany

[b] Microbial Biotechnology, Faculty of Biology and Biotechnology
Ruhr-University Bochum
Universitätsstraße 150, 44780 Bochum, Germany

[c] Department of Biotechnology
Delft University of Technology
Van der Maasweg 9, 2629 HZ Delft, The Netherlands

[d] Department of Biocatalysis
Institute of Catalysis and Petrochemistry (CSIC)
Campus Cantoblanco, 28049 Madrid, Spain

[e] current address:
Institute for Molecular Biotechnology
Graz University of Technology
Petersgasse 14, Graz, Austria

* Corresponding author: Julia E. Bandow, julia.bandow@rub.de

Supporting information for this article is given via a link at the end of the document.

Abstract

Peroxidases and peroxygenases are promising classes of enzymes for biocatalysis because of their ability to carry out one-electron oxidation reactions and stereoselective oxyfunctionalizations. Industrial application is however limited, as the major drawback is the sensitivity towards the required peroxide substrates. Herein, we report a novel biocatalysis approach to circumvent this shortcoming: *in situ* production of H_2O_2 by dielectric barrier discharge plasma. The discharge plasma can be controlled to produce hydrogen peroxide at desired rates yielding desired concentrations. Using horseradish peroxidase, we demonstrated that hydrogen peroxide produced by plasma treatment can drive the enzymatic oxidation of model substrates. Fungal peroxygenase was then employed to convert ethylbenzene to (*R*)-1-phenylethanol with an *ee* of >96 % using plasma-generated hydrogen peroxide. Since direct treatment of the reaction solution with plasma resulted in reduced enzyme activity, the use of plasma-treated liquid and protection strategies were investigated to increase total turnover. Technical plasmas present a non-invasive means to drive peroxide-based biotransformations.

Introduction

Cold plasmas have a variety of different applications, ranging from surface preparation in material sciences to treating skin infections in plasma medicine.[1–3] In general, plasmas are generated by accelerating free electrons by applying an electric field to ambient air or a defined gas mixture. Collisions of high-temperature electrons with atoms or molecules in the gas phase lead to the formation of excited species, radicals, and metastables, which in turn react to form other species. In fact, for ambient air over 600 different reaction mechanisms are postulated.[4] Because the electric field provides the light electrons with high kinetic energy, but not the heavier particles, the overall temperature of the plasma is ambient (hence the term non-thermal plasma). The plasma-generated species as well as the UV-photons stemming from the relaxation of excited species are able to interact with gases or liquids exposed to the plasma. One of the species generated in high amounts in plasma-treated liquids is hydrogen peroxide (H_2O_2)[5], which can be a valuable oxidant for enzymatic conversions.

Peroxidases and peroxygenases are heme-containing enzymes that upon activation by H_2O_2 can perform a multitude of natural functions, e.g. condensation of biopolymers[6], immune defense[7], or detoxification of highly reactive H_2O_2[8]. However, peroxidases, which perform one-electron oxidations, and especially peroxygenases (performing both one-electron oxidations and most remarkably, two-electron oxidation reactions) are also remarkable enzymes for different biotechnological purposes. In particular, the 2-electron C-H oxyfunctionalization reactions carried out by peroxygenases are raising great interest for synthetic chemistry.[9] Nevertheless, using these biocatalysts on a larger scale is challenging, mainly because the substrate H_2O_2 also leads to inactivation of the enzymes when present at high concentrations.[10] In a commercial setting, this would require enzyme replacement after few reaction cycles or it would lead to strong dilution of the reaction solution if H_2O_2 is added at low concentrations. Both strategies are typically little profitable. An alternative to using stock solutions is the generation of H_2O_2 *in situ*. To this effect, several different strategies have been developed, such as the use of enzyme cascades[11,12], light activated flavins[13–15], or photocatalysts[16–18]. All of these strategies require the addition of extra components to the reaction, incurring additional costs, especially in the case of enzymes and flavins. Another approach uses immersed electrodes and electrochemistry to produce H_2O_2.[19–22] While this system does not rely on the addition of components to the solution, electrodes are immersed which may trigger precipitation of buffer salts and enzymes. A non-invasive *in situ* approach that allows to control H_2O_2 levels would present a significant advantage.

Here, we report on the use of a novel, non-invasive approach to fuel H_2O_2-based biotransformations: the *in situ* generation of H_2O_2 using a dielectric barrier discharge (DBD) plasma (Fig. 1). The DBD device is operated in a surface discharge mode so that only the plasma comes into contact with the reaction solution. Plasma parameters are readily tunable and can be tailored to the needs of the enzyme employed. For instance, frequency, voltage, and power density influence H_2O_2 production and can be adjusted.[23] With regard to temperature reaction conditions are mild since the non-thermal plasma used here causes negligible heating.[24] A proof-of-principle study was performed with horseradish peroxidase

(HRP) and the model substrate guaiacol. Plasma stability of the enzyme, optimal plasma parameters, and plasma-triggered side reactions were investigated. Enzyme protection strategies were tested, including protein immobilization, which, by placing enzymes at a distance from the plasma-liquid interface, protects proteins from the most reactive species. The biotechnological potential with regard to selectivity was evaluated using the evolved recombinant unspecific peroxygenase from *Agrocybe aegerita* (r*Aae*UPO), one of the most promising enzymes for peroxide-dependent oxyfunctionalization chemistry.[25]

Results and Discussion

Proof of principle

The concept of plasma-driven biocatalysis is illustrated in Fig. 1. DBD plasmas induce formation of reactive oxygen and nitrogen species (RONS), including H_2O_2. Peroxidases or peroxygenases then utilize the supplied H_2O_2 to produce valuable products from precursors, i.e. oxidized organic substances.

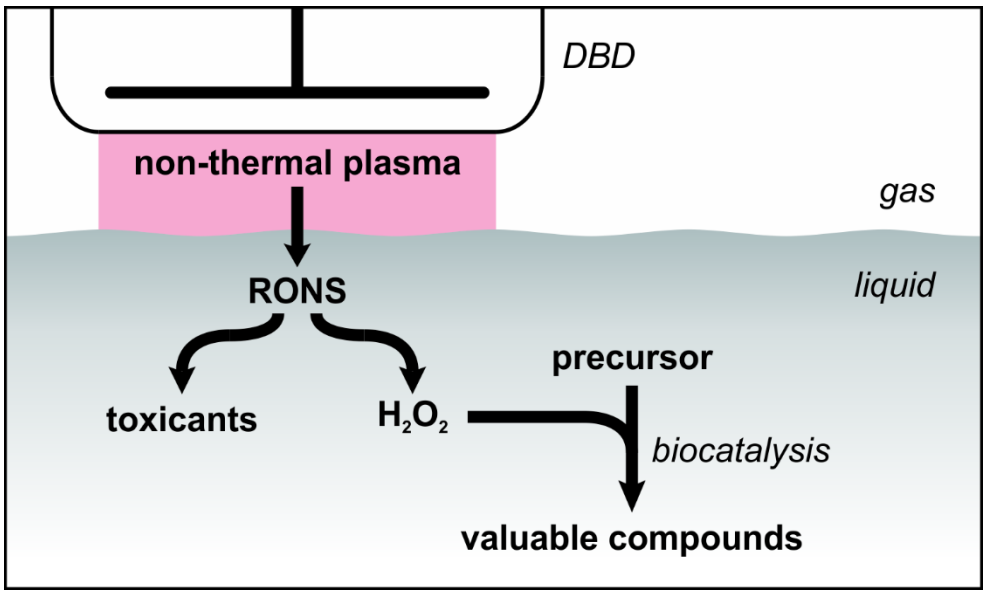

Figure 1. General scheme of plasma-driven biocatalysis. A dielectric barrier discharge is generating a non-thermal plasma that interacts with the liquid, thus forming reactive oxygen and nitrogen species (RONS), e.g. peroxynitrite ($ONOO^-$), superoxide ($O_2^{\cdot-}$), or H_2O_2. Some of

the species can further react to other reactive particles, most of which represent toxicants. Other species such as H_2O_2, however, can serve as a reactant to fuel biocatalysis.

The DBD device used in this study can be ignited in air, eliminating the need for expensive feed gases like helium or argon, which are commonly used to operate other plasma devices. Also, the source generates H_2O_2 in the treated liquid at rates adequate for the enzymes employed here. HRP was used as the model enzyme in the proof-of-principle experiment since it is well-studied, highly stable, and commercially available.[26–28] Without further purification (Rz>2.5), HRP was dissolved in phosphate buffer and, after addition of the chromogenic substrate guaiacol, treated directly with the DBD device operated in ambient air (Fig. 2). In the presence of H_2O_2, HRP oxidizes guaiacol to tetraguaiacol which exhibits an A_{max} at λ = 470 nm. With increasing treatment time, A_{470} rises, indicating successful production of tetraguaiacol. Plasma treatment of guaiacol alone or incubation of HRP with guaiacol without plasma treatment did not result in tetraguaiacol production (Supplementary Fig. 1). When inactivated HRP (HRP from which heme had been extracted with ethyl acetate) was used, no product was observed either, indicating that enzyme activity is strictly required for guaiacol conversion (Supplementary Fig. 2). H_2O_2 concentration was measured concomitantly and was found to increase linearly by approximately 0.1 mM min^{-1} for the reaction volume tested here. This is in agreement with previous reports on plasma-based H_2O_2 production.[29]

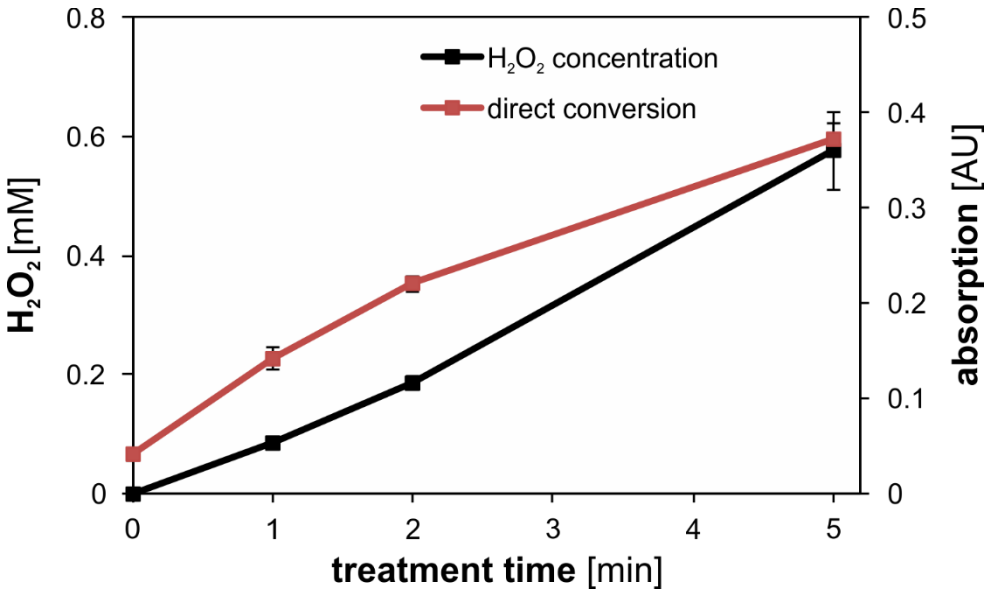

Figure 2. Kinetics of H_2O_2 accumulation and substrate conversion by HRP during direct plasma treatment with the CINOGY PlasmaDerm DBD device. Samples were placed onto glass slides and treated for the indicated amount of time. Black: 100 µl of 50 mM KPi buffer were treated with plasma. Immediately after treatment, 20 µl of the samples were mixed with 180 µl *A. dest.* and H_2O_2 concentrations determined using the Spectroquant Hydrogen Peroxide kit (Merck) and photometrical measurements at 455 nm. Red: direct conversion of guaiacol (5 mM) with plasma was carried out by treating 100 µl of KPi buffer containing 0.1 U ml^{-1} HRP. Production of tetraguaiacol was followed at λ = 470 nm. The data shown represents means of three independent experiments.

HRP inactivation mechanisms

While the H_2O_2 supply is steady for the treatment times tested, the tetraguaiacol production rate declines at prolonged exposure (Fig. 2). The observed decrease in tetraguaiacol production rates at 5 min could be caused by degradation of the enzyme or further modification of the product during plasma exposure. Indeed, the absorption spectrum of the plasma-generated biocatalysis product of guaiacol conversion differed from the product formed with exogenously added H_2O_2 (Supplementary Fig. 3). For alternative HRP substrates pyrogallol and L-DOPA we observed oxidation to the final product by plasma treatment even in the absence of enzyme (Supplementary Fig. 4).

Inactivation of enzymes with the plasma source used here was shown before, e.g. with RNase A which was fully inactivated after 5 min of treatment.[29] Activity loss of heme-containing proteins, and specifically HRP, has also been studied[30–32], albeit not with the plasma device used here. When treated with an argon discharge, HRP was fully inactivated within 30 min. However, the plasma device used in this work was specifically designed for use in dermatology[33] and could be characterized by slower inactivation kinetics. It is worth mentioning here that it depends on the enzyme how deleterious the effects of plasmas are. Some enzymes even exhibited increased activity after plasma treatment.[34,35]

In order to assess HRP inactivation by the plasma treatment performed in this work, HRP was treated with the DBD plasma and activity determined subsequently *ex situ* with a defined amount of H_2O_2 (Fig. 3). HRP activity decreased with increasing plasma treatment time, resulting in only residual activity after 10 min of treatment. HRP inactivation was found to be largely independent of protein concentration during treatment (Supplementary Fig. 5).

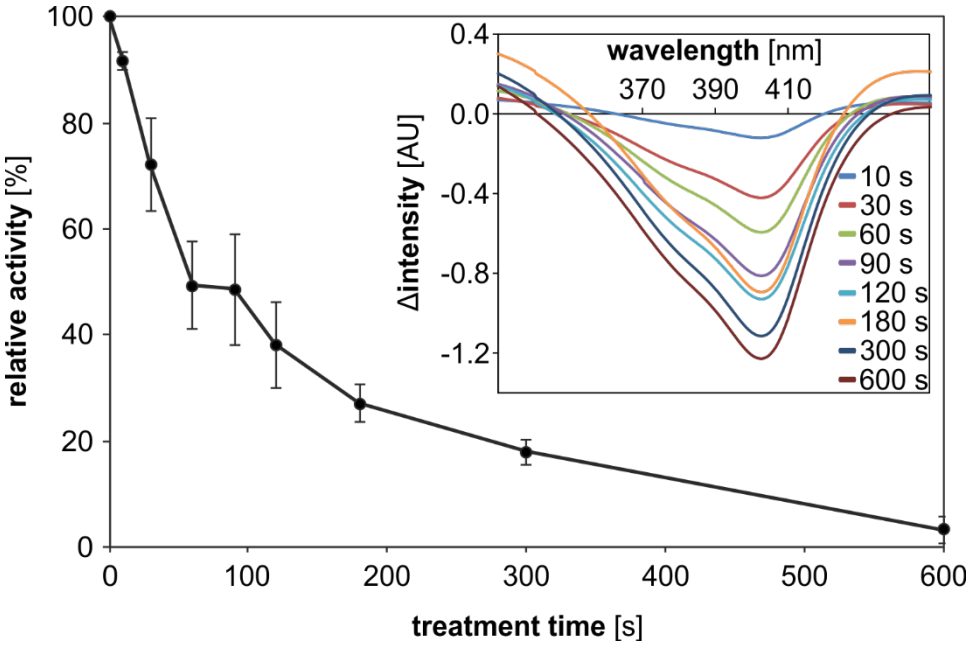

Figure 3. HRP inactivation by plasma treatment. Plasma treatment was performed with 110 µl 1 kU ml^{-1} HRP in KPi (100 mM, pH 6.5) buffer without guaiacol. Activity was measured by diluting the treated samples to 0.1 U ml^{-1} in KPi buffer including 5 mM of guaiacol and subsequent addition of H_2O_2 at a final concentration of 0.25 mM. Guaiacol conversion was

immediately monitored at λ = 470 nm and activity calculated from the initial slope during the first 30 s. From the same treated samples, absorption spectra were measured with a 1:5 dilution in KPi. The inset shows the Soret band of HRP with A_{max} at ~ 403 nm. Spectra are displayed with the untreated sample as blank, thereby showing a decrease of absorbance at the Soret peak. Data was recorded in triplicates for both activity measurements and spectra.

HRP depends on a heme cofactor for activity that absorbs at λ ~ 403 nm (Soret band). To assess integrity of the heme cofactor, absorption spectra were recorded for the protein samples that were tested for activity (inset of Fig. 3). In congruence with previous reports[30], absorption of the Soret band declined after plasma exposure, indicating that the heme is modified. Heme has been shown to be attacked by ROS, e.g. O_2^- radicals and H_2O_2[36,37], both of which represent major components of the discharge and the treated liquid. H_2O_2 is needed as a substrate for the peroxidation reaction, but O_2^- may only act as toxicant. We attempted to eliminate O_2^- radicals using superoxide dismutase A (SodA) from *Escherichia coli*, an enzyme that converts O_2^- to H_2O_2. Superoxide dismutases are among the fastest enzymes, operating near the diffusion limit of substrate supply.[38,39] SodA was added to the reaction solution prior to plasma treatment. No difference in catalytic efficiency of HRP was observed (Supplementary Fig. 6). Therefore, we conclude that either the concentration of O_2^- in plasma treated samples is insignificant for heme degradation or that SodA is immediately inactivated by plasma-generated species and thus cannot provide protection to HRP.

Heme-binding can also induce conformational changes in apoproteins.[40] Since it was shown previously that plasma discharges can impact the structural integrity of proteins[29,31,41,42], we investigated the structure of HRP upon plasma exposure using circular dichroism (CD) spectroscopy (Fig. 4). No conformational changes of HRP were detected even at treatment times of 5 min which render HRP largely inactive. This indicated that damage to the heme moiety did not negatively affect HRP structure. The fact that no structural changes were observed also allowed conclusions on another structural feature, namely disulfide bonds. HRP contains eight cysteines, all of which are engaged in disulfide bonds, that contribute to the high

enzyme stability.[26] For RNase A, a highly stable enzyme with four disulfide bonds, oxidation of cysteines to their sulfenic and sulfonic acids was observed upon DBD treatment which resulted in significant unfolding.[29] If such amino acid modifications also occurred in HRP, they did not seem to affect the overall protein fold.

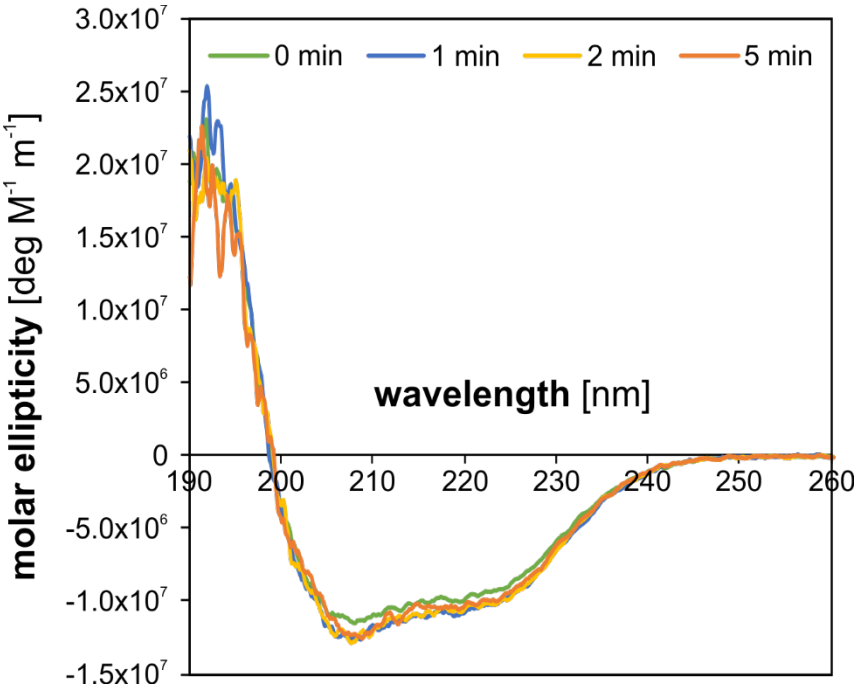

Figure 4. CD spectra of HRP after exposure to plasma. 110 µl HRP were treated as described above for activity measurements and diluted 1:5, which corresponds to 0.2 mg ml^{-1} for the untreated sample. Immediately after treatment, the sample was transferred to a suitable cuvette and subjected to CD measurements. CD spectra were normalized with respect to protein concentration as determined by the Bradford method.

The specific heme content (heme per protein) of peroxidases is defined by the Rz value (A_{403}/A_{275}). Because plasma-generated species also absorb in the UV region[43], specific heme content in this case was calculated as the quotient of A_{403} and protein concentration as measured by Bradford assay (Fig. 5). Dependent on the plasma exposure time, protein concentration decreased. This phenomenon was observed previously for HRP as well as other enzymes treated in aqueous solution, e.g. hemoglobin, myoglobin, and BSA.[31,44] In fact, it has been shown that treatment with the plasma source used in this study leads to the cleavage of

peptide bonds and thus protein degradation[44]. This protein degradation was partially inhibited by the addition of mannitol, which had been described as •OH scavenger.[45] Protein fragmentation will lead to activity loss. However, since the CD spectra indicate that the structure of the HRP remaining after 5 min treatment was still intact and the rate of heme degradation for HRP exceeded the decrease in HRP concentration, we conclude that heme damage, rather than structural changes or protein degradation, is the primary cause for HRP inactivation.

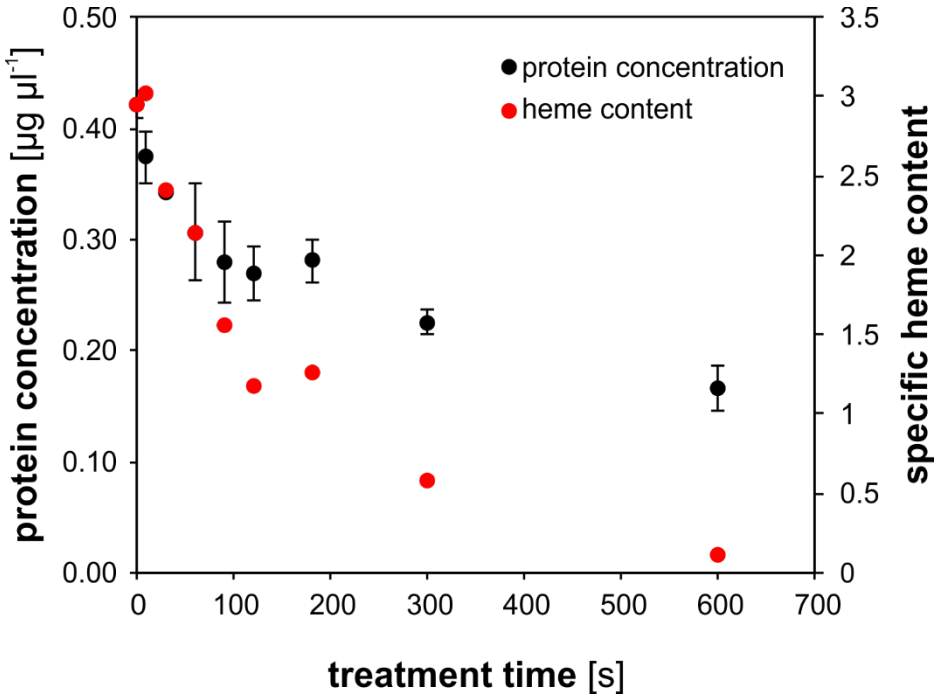

Figure 5. Decrease in protein concentration and heme content. Protein concentration was determined using the Bradford method. Specific heme content was set as absorbance at λ = 403 (see Fig. 3) divided by protein concentration and displayed in arbitrary units. Protein concentration was determined in triplicates.

Optimizing plasma treatment conditions

For the proof of concept study with HRP, the parameters for plasma operation (pulse amplitude 13.5 kV, trigger frequency 300 Hz) were chosen simply by applying the same parameters as in previous studies.[29,46] In an effort to optimize operating conditions for longevity of HRP, a range of amplitudes and frequencies between 11.5 and 17.5 kV and 150 and 700 Hz,

respectively, was tested (Fig. 6). To this end, HRP activity was measured immediately after 1 min of plasma treatment. The activity measurement was decoupled from plasma treatment of the enzyme-containing solution in order to circumvent the issue of plasma-induced product modification discussed above (Fig. 2) that may obstruct interpretation of the results. Changes in trigger frequency showed little to no effect on HRP activity (Fig. 6), while HRP inactivation increased with increasing applied voltage. A very similar dependency of protein activity on discharge voltage was shown previously for tomato peroxidase, even with similar kinetics, although a different DBD plasma was used.[47]

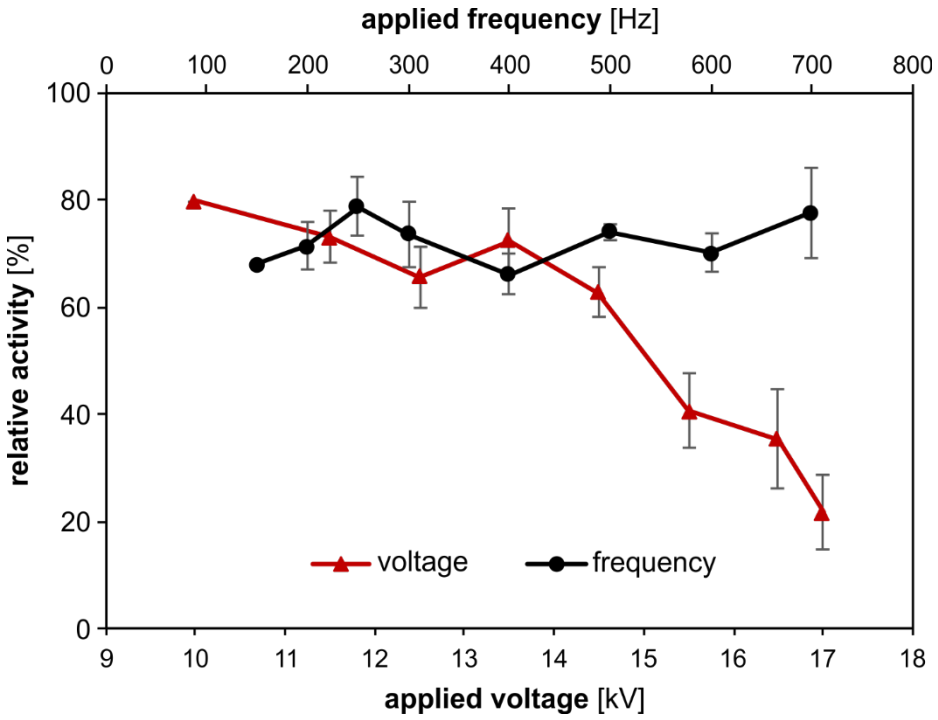

Figure 6. Influence of voltage and frequency on HRP after 1 min of plasma treatment. HRP was plasma-treated at 10 U ml^{-1} for 1 min and activity was subsequently measured *ex situ* as described above. Untreated samples were set to 100%. The graph shows mean values of three independent replicates.

An increase in applied voltage leads to higher electron temperatures in the gas phase and in turn increased ROS production, so that a higher density of toxicants is expected in the liquid. It was for instance shown previously that •OH production in plasma-treated liquid depends on

the specific energy transferred, which can be manipulated either by treatment time or by the voltage applied.[23] Addition of the •OH scavenger mannitol during plasma treatment did not have a significant effect on HRP lifetime (Supplementary Fig. 7). We speculate that other RONS such as atomic oxygen (•O), UV radiation, and/or the applied electric field[48,49] might impact enzyme activity.

Another approach to extending HRP lifetime was immobilization of the enzyme to non-reactive support beads. Immobilization was carried out by reacting HRP with glutaraldehyde-activated polymer beads. Immobilized HRP exhibited only ~10% of the activity of the free enzyme (Supplementary Fig. 8). However, when plasma treated, $HRP_{immobilized}$ retained its activity significantly longer. After 5 min of treatment, immobilized HRP showed 41.8% activity compared to the untreated $HRP_{immobilized}$, while free enzyme activity was reduced to 0.5% to 10% (results presented in Fig. 7 and Fig. 3, respectively).

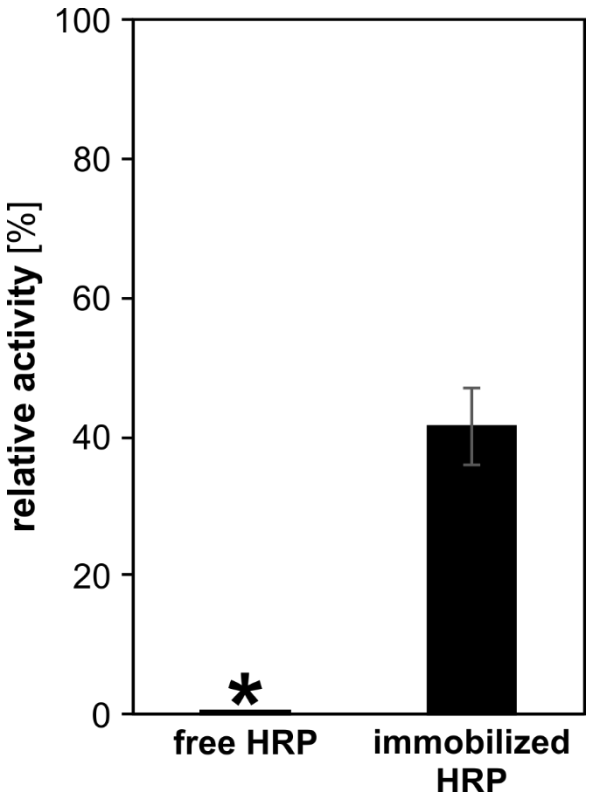

Figure 7. Immobilization of HRP protects against plasma-mediated damage. Glutaraldehyde-activated polymethacrylate beads (Relizyme HA403) were incubated with HRP over night to yield an immobilized HRP solution corresponding to 20 U ml^{-1}. For both enzyme formulations,

100 µl were treated at 13.5 kV and 300 Hz. Free enzyme activity was measured as described above. Activity assays for immobilized HRP were conducted with constant shaking to provide sufficient substrate delivery to the macroscopic beads, using 5 mM guaiacol and 0.25 mM H_2O_2. The displayed relative activities were calculated by relating the activities of treated samples to their respective untreated controls. Data represent means of three replicates.

The comparably high robustness of immobilized enzyme might be attributed to spatial separation. Most recombination reactions in plasma-treated liquids are thought to occur at or in close proximity to the liquid-gas interface.[50] RONS like singlet oxygen ($^1\Delta_gO_2$), O_2^-, and •OH have average diffusion distances in the nm-µm range.[51] The liquid droplets in our experimental setup are approximately 2 mm in height and the protein-loaded beads sink to the bottom of the sample. This creates a protein-free buffer zone that allows most short-lived toxicants to react and form less harmful species before they can interact with the protein. However, the recombination reactions at the plasma-liquid interface are experimentally very challenging to address. Most studies, therefore, address this question based on numerical modelling (reviewed in [52]). According to the models, many of the reactive species have short lifetimes in the liquid phase, e.g. in the ns-µs range for •OH. Thus, a spatial gradient forms in the liquid phase such that the more reactive species penetrate less deep before they react further.[53,54] The models are congruent with a mm of liquid column being sufficient to protect proteins from exposure to the most reactive species.

Selectivity in plasma-driven biocatalysis

In order to assess the potential of plasma-driven biocatalysis, we felt it necessary to investigate if plasma-based H_2O_2 production interferes with the stereoselectivity of enzymatic reactions. To this end, the r*Aae*UPO was used, an enzyme capable of performing stereoselective oxidations of hydrocarbons.[12,55] For r*Aae*UPO, total turnover numbers (TTNs) of >10,000 have been reported, indicating its remarkable stability.[56–58] As model reaction we chose the well-characterized oxidation of ethylbenzene to (*R)*-1-phenylethanol, a reaction that would provide

proof that a value-adding reaction can be driven by plasma. First, H_2O_2 was generated by treating a set volume of 100 µl KPi buffer with plasma for 5 min and then adding it to a solution containing r*Aae*UPO and ethylbenzene (indirect treatment). After 10 min reaction time, another 100 µl of treated buffer were added, and after further 10 min reaction time, another 100 µl of treated buffer were added prior to allowing a final 10 min reaction time. Formation of (*R)*-1-phenylethanol was determined, yielding a final concentration of 0.46 mM (Table 1).

Table 1. Production of (*R)*-1-phenylethanol from ethylbenzene starting with a solution of 1 µM r*Aae*UPO and 5 µl of ethylbenzene. 100 µl increments of buffer solutions were treated for the indicated amounts of time and added to the reaction solution. After 10 min of incubation under agitation, the next increment of treated buffer was added. In total, three increments were added per sample. TON: turnover number. Data represent means and standard deviations of three replicates.

treatment time per increment [min]	**buffer composition**	**final (*R)*-1-phenylethanol concentration [mM]**	**TON**
0	KPi 250 mM	0	0
5	KPi 250 mM	0.46 ± 0.01	4576
10	KPi 250 mM	0.69 ± 0.25	6935
15	KPi 250 mM	0.97 ± 0.17	9709
20	KPi 250 mM	1.38 ± 0.13	13787
5	KPi 1 M	0.83 ± 0.06	8279
5	KPi 50 mM	0.7 ± 0.03	6993
5	Tris 50 mM	0.92 ± 0.01	9170
5	HEPES 50 mM	1.35 ± 0.03	13493
5	MES 50 mM	0.78 ± 0.01	7831

Treatment times for each increment were then varied to change H_2O_2 concentrations. Product formation was linearly correlated with the treatment time. The calculated turnover number of 13,787 indeed is on the order of previously reported TTNs of r*Aae*UPO.[55] Negative controls

without enzyme, plasma treatment, or ethylbenzene did not result in any detectable product formation (Supplementary Fig. 9). The product was optically pure with an *ee* ranging between 96 % to >99 %, which clearly demonstrates that the hydroxylation is indeed an enzymatic reaction (Supplementary Fig. 9). We also tested whether other long-living RONS present in plasma-treated buffer have an impact on r*Aae*UPO activity. The enzyme was added to plasma-treated buffer or to H_2O_2 diluted to the same concentration as detected in the plasma-treated sample. After 2 min incubation, substrate was added and the enzyme activity assay performed using only the H_2O_2 already present in the sample (Supplementary Fig. 10). There was no difference in enzyme inactivation rates, showing that other long-living plasma-induced species, such as $ONOO^-$ or NO_2, do not have a significant effect on enzyme lifetime.

Different buffer salts were tested for their influence on the reaction yield. The best results were obtained with HEPES buffer yielding about twice as much product than with KPi, followed by MES buffer and Tris buffer (Tab. 1). It has been reported that UV-irradiated HEPES produces H_2O_2, which may be one possible explanation for the observed increase since the employed plasma source emits UV photons.[59] Another possible explanation is that plasma-generated peroxynitrite (from the reaction of O_2^- and •NO) can react with HEPES to form H_2O_2.[60]

Having established that plasma-treated buffer is a suitable source of H_2O_2 for biocatalysis with r*Aae*UPO, we investigated suitability of r*Aae*UPO for direct plasma-driven biocatalysis. 100 µl of 1 µM enzyme in 250 mM KPi buffer was mixed with 5 µl of ethylbenzene and plasma-treated for 5 min, yielding 0.05 mM of (*R)*-1-phenylethanol. Compared to supplying H_2O_2 from plasma-treated KPi buffer incrementally, plasma-driven biocatalysis gave a 11 % yield, indicating either enzyme inactivation, substrate limitation (the substrate is poorly soluble in aqueous solution and forms an organic phase on top of the reaction solution), or degradation of the product (*R)*-1-phenylethanol by short-lived plasma species. Like HRP, r*Aae*UPO relies on a heme cofactor. Inactivation kinetics of r*Aae*UPO were similar to those of HRP (Supplementary Fig. 11). The addition of *E. coli* SodA also did not have a significant effect on the lifetime of r*Aae*UPO when exposed to plasma (Supplementary Fig. 12). And like for HRP, when r*Aae*UPO was immobilized using the same carrier, the relative activity after plasma treatment compared to

untreated samples was significantly higher than for the free enzyme (Supplementary Fig. 11 and 13). Immobilized r*Aae*UPO retained approx. 39% activity compared to the free enzyme (Supplementary Fig. 14), indicating that immobilization has less of an impact on enzyme activity than for HRP (approximately 10% activity after immobilization (Supplementary Fig. 8)). However, when immobilized r*Aae*UPO was directly treated in-solution in the presence of ethylbenzene for 5 min, no product was formed. Since the enzyme still showed 75% activity after 5 min of plasma exposure (Supplementary Fig. 13), we attribute the lack of conversion to substrate limitation, possibly caused by poor substrate solubility and insufficient mixing or by evaporation of the ethylbenzene during the treatment.

To overcome the limits of the direct exposure (presumably the substrate limitation) while retaining the benefit of the *in situ* approach of keeping the final volume constant, *ex situ* plasma-treatment was combined with the use of immobilized r*Aae*UPO (Fig. 8). After the addition of the substrate, a volume of 100 µl of the solution from the liquid column above the beads was taken from the vial, treated with the DBD for 5 min, and returned to the reaction. Using this strategy, the same amount of product was obtained as for the addition of plasma-treated buffer, but without diluting the reaction solution. For reactions with poorly soluble substrates, the *ex situ* treatment of reaction solutions thus presents a viable option with the decisive advantage of avoiding sample dilution in synthetic applications.

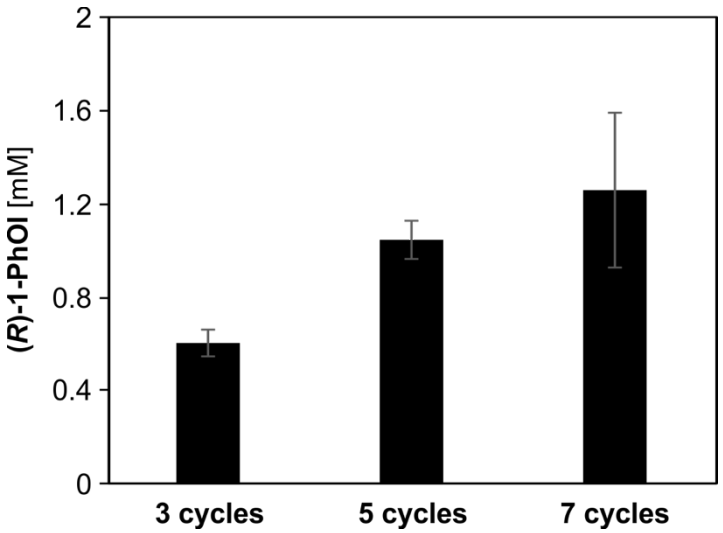

Figure 8. Production of (*R)*-1-phenylethanol with immobilized r*Aae*UPO using plasma-treated KPi buffer (250 mM) treated for several cycles. Supernatant of the reaction vial, i.e. buffer without enzyme, was treated as mentioned before and added back to the container. This was repeated for several cycles as indicated. Turnover of ethylbenzene to (*R*)-1-phenylethanol was allowed to take place for 30 min after a new cycle was initiated. (*R*)-1-PhOl: (*R*)-1-phenylethanol.

The product obtained using immobilized r*Aae*UPO and several cycles of plasma-treated buffer presented an *ee* of > 99 %, indicating that the plasma treatment did neither modify nor racemize (*R*)-1-phenylethanol, nor did it change selectivity of the enzyme. Up to seven treatment cycles were tested, resulting in an accumulation of (*R*)-1-phenylethanol to concentrations of up to 1.26 mM, which is in the range of product obtained with 60 min cumulated treatment time in the *ex situ* approach (Tab. 1). To investigate if immobilized r*Aae*UPO that was exposed to plasma-treated liquids can be reused, the supernatant was extracted before new plasma-treated buffer and substrate were added. In all of the 8 cycles the same amount of *(R)*-1-phenylethanol was generated (Supplementary Fig. 15), indicating that enzyme activity is not impaired by repeated exposure to plasma-treated buffer.

Conclusion

In this work, we present the first non-invasive *in situ* method to generate H_2O_2 for biocatalysis using a cold plasma device. Advantageous to this system is the ability to fine-tune the H_2O_2 production rate without changing the setup. We show that limitations in enzyme stability under direct plasma treatment of the reaction solution can be overcome by enzyme immobilization. Plasma-driven biocatalysis may present a path forward for peroxidase and peroxygenase catalyzed stereoselective oxyfunctionalization reactions. Furthermore, our results suggest that enzyme immobilization is a useful tool for studying the interaction mechanisms of plasma, liquids, and proteins.

Experimental Section

Enzymes

HRP was purchased from Sigma (P8375, Rz > 2.5) and stored in 100 mM KPi, pH 6.5. SodA (Uniprot P00448) was obtained from an *E. coli* strain harbouring a His6-*sodA* fusion plasmid (*E. coli* BL21 DE3 pASK-IBA+::*his6-sodA*) by following standard protocols for cultivation, cell lysis, and purification as described in the supporting information. r*Aae*UPO (Uniprot B9W4V6) was purified as described before.[61] Briefly, culture supernatant of a *Pichia pastoris* strain expressing r*Aae*UPO and secreting it into the culture medium was subjected to micro-filtration prior to use.

Plasma source and treatment

The plasma source used for all experiments was the CINOGY PlasmaDerm system (CINOGY, Duderstadt, Germany). For a detailed review of the plasma source, including power calculations, see[33]. Unless indicated otherwise, all plasma treatments were performed with standard conditions at room temperature and in ambient air: electrode diameter, 20 mm; pulse amplitude, 13,5 kV; trigger frequency, 300 Hz. Plasma exposure of liquid samples of 110 µl volume was performed using PTFE-coated glass slides. Since plasma treatment increases hydrophilicity of the glass surface, the liquid was contained in PTFE wells to prevent spreading. Distance between dielectric and sample apex was kept constant at approximately 2 mm for all samples. All subsequent analyses were performed immediately after treatment unless noted otherwise.

H_2O_2 measurement

Samples were analysed and calibrated with a commercially available test kit following the manufacturer's instructions (Spectroquant Hydrogen Peroxide, Merck). After a 10 min reaction time, absorption at 455 nm was measured. Calibration was performed with serial dilutions from 0-200 µM made from H_2O_2 stock.

Ex-situ activity assays

HRP was added to a guaiacol solution in 100 mM KPi (pH 6.5). To start the reaction, the same volume of 1 mM H_2O_2 was added and the absorption at 470 nm immediately monitored with a plate reader (Biotek µQuant, Bad Friedrichshall, Germany). Final concentrations were usually 0.1 U ml^{-1} HRP, 5 mM guaiacol, 50 mM KPi, and 0.5 mM H_2O_2. For r*Aae*UPO activity measurements, 2,2'-azino-bis(3-ethylbenzothiazoline-6-sulphonic acid) (ABTS) was used as chromogenic substrate. Final concentrations in this case were 40 nM r*Aae*UPO, 2.5 mM ABTS, 50 mM sodium acetate buffer (pH 5.5), and 1 mM H_2O_2. Activity was determined based on the slope of the linear region of the absorption measurement plot.

CD spectroscopy

HRP was treated as described above and immediately mixed with four parts of 100 mM KPi. After transfer to a cuvette, CD spectra were recorded with a Jasco J-815 CD spectrometer (Jasco, Pfungstadt, Germany) with the following parameters: range, 190-300 nm; data interval, 0.1 nm; bandwidth, 2 nm; accumulations, 5. KPi buffer was used as blank. Samples were then extracted from the cuvette and subjected to a Bradford assay performed according to manufacturer's instructions (RotiNanoquant Kit, Roth, Karlsruhe, Germany). The ellipticity was corrected for the protein concentration as described before.[62]

Immobilization

HRP and r*Aae*UPO were immobilized with Relizyme HA403 M beads (Resindion, Binasco, Italy). To this end, 10 mg of beads were activated by incubating in KPi buffer (pH 7) with 0.4% glutaraldehyde for 1 h. After washing twice with deionized water, up to 5 mg of enzyme were

added in 1 ml buffer. Immobilization was carried out overnight at room temperature under constant shaking. Binding efficiency was determined by measuring the protein concentration in the supernatant after incubation and was found be >80% in all cases.

Analysis of r*Aae*UPO catalysis products

Buffer volumes of 110 µl were treated with the DBD plasma as described for HRP for different amounts of time. Treated buffer was then allowed to rest for five minutes for short-lived reactive species to react. 100 µl of this treated buffer was combined with 5 µl of ethylbenzene and 50 µl of a 1 µM r*Aae*UPO solution and incubated for 10 min at 30 °C and 600 rpm. Then, another 100 µl of treated buffer was added and the reaction was incubated for another 10 minutes. This was followed by a third addition of treated buffer and incubation. The final reaction volume (355 µl) was extracted with 300 µl ethyl acetate containing 2 mM of 1-octanol as injection standard. The organic phase was dried with $MgSO_4$ and measured with a Shimadzu 2010 1 system containing a Hydrodex β-6TBDM column (Macherey-Nagel, Germany). The column was heated at 120 °C for 20 minutes. Final concentrations of (*R)*-1-phenylethanol were determined by applying a standard curve that was measured with racemic 1-phenylethanol.

Acknowledgements

We thank Cinogy for kindly providing the plasma source and Britta Schubert for technical assistance. We gratefully acknowledge funding by the German Research foundation to JEB (CRC1316-1 and BA 4193/7-1).

Keywords: biocatalysis • peroxidase • peroxides • peroxygenase • plasma chemistry

10.1002/cssc.201903438

Table of contents

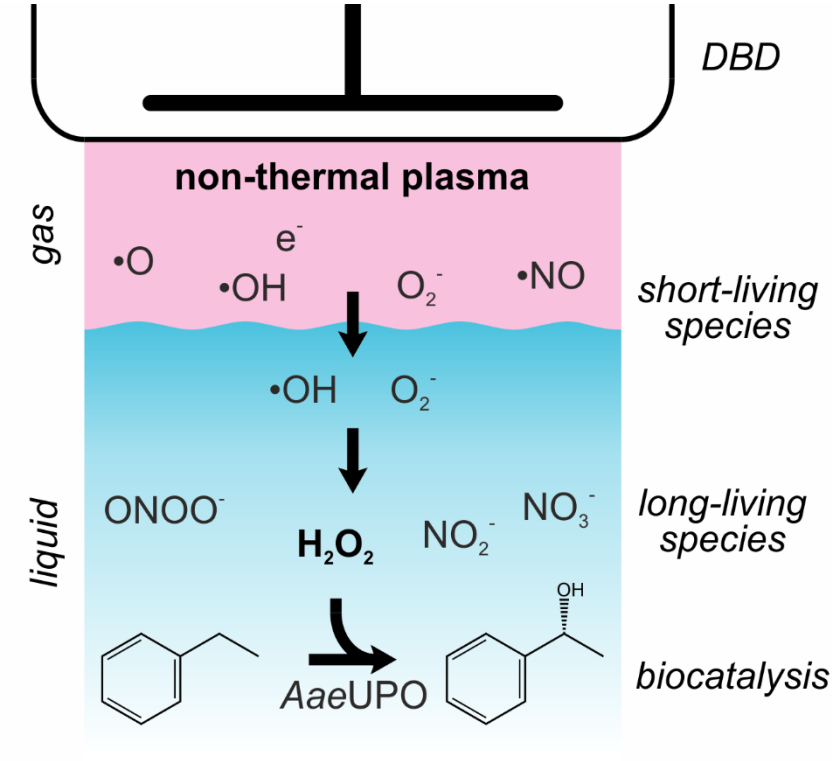

Ride the lightning: Non-thermal plasma was applied for non-invasive production of hydrogen peroxide to be used in biocatalysis. Side effects of plasma exposure can be alleviated by enzyme immobilization. Enantiomerically pure (*R*)-1-phenylethanol was produced with plasma-generated H_2O_2 and *Aae*UPO.

References

[1] E. R. Fisher, *Plasma. Process. Polym.* **2004**, *1*, 13.

[2] R. Morent, N. Geyter, T. Desmet, P. Dubruel, C. Leys, *Plasma. Process. Polym.* **2011**, *8*, 171.

[3] B. Haertel, T. Woedtke, K.-D. Weltmann, U. Lindequist, *Biomol. & Ther.* **2014**, *22*, 477.

[4] Y. Sakiyama, D. B. Graves, H.-W. Chang, T. Shimizu, G. E. Morfill, *J. Phys. D: Appl. Phys.* **2012**, *45*, 425201.

[5] F. Judée, S. Simon, C. Bailly, T. Dufour, *Water Res.* **2017**, *133*, 47.

[6] S. Sasaki, T. Nishida, Y. Tsutsumi, R. Kondo, *FEBS Lett.* **2004**, *562*, 197.

[7] B. S. van der Veen, M. P. J. Winther, P. Heeringa, *Antioxid. Redox. Signal.* **2009**, *11*, 2899.

[8] B. N. Tripathi, I. Bhatt, K.-J. Dietz, *Protoplasma* **2009**, *235*, 3.

[9] B. O. Burek, S. Bormann, F. Hollmann, J. Z. Bloh, D. Holtmann, *Green Chem.* **2019**, *21*, 3232.

[10] B. Valderrama, M. Ayala, R. Vazquez-Duhalt, *Chem. Biol.* **2002**, *9*, 555.

[11] D. Jung, C. Streb, M. Hartmann, *Microporous Mesoporous Mat.* **2008**, *113*, 523.

[12] Y. Ni, E. Fernández-Fueyo, A. Gomez Baraibar, R. Ullrich, M. Hofrichter, H. Yanase, M. Alcalde, W. J. H. van Berkel, F. Hollmann, *Angew. Chem. Int. Ed. Engl.* **2016**, *55*, 798.

[13] M. Girhard, E. Kunigk, S. Tihovsky, V. V. Shumyantseva, V. B. Urlacher, *Biotechnol. Appl. Biochem.* **2013**, *60*, 111.

[14] I. Zachos, S. K. Gassmeyer, D. Bauer, V. Sieber, F. Hollmann, R. Kourist, *Chem. Commun.* **2015**, *51*, 1918.

[15] D. I. Perez, M. M. Grau, I. W. C. E. Arends, F. Hollmann, *Chem. Commun.* **2009**, 6848.

[16] Y. Shiraishi, S. Kanazawa, D. Tsukamoto, A. Shiro, Y. Sugano, T. Hirai, *ACS Catal.* **2013**, *3*, 2222.

[17] W. Zhang, B. O. Burek, E. Fernández-Fueyo, M. Alcalde, J. Z. Bloh, F. Hollmann, *Angew. Chem. Int. Ed. Engl.* **2017**, *56*, 15451.

[18] S. J.-P. Willot, E. Fernández-Fueyo, F. Tieves, M. Pesic, M. Alcalde, I. W. C. E. Arends, C. B. Park, F. Hollmann, *ACS Catal.* **2019**, *9*, 890.

[19] K. Lee, S.-H. Moon, *J. Biotechnol.* **2003**, *102*, 261.

[20] C. Kohlmann, S. Lütz, *Eng. Life Sci.* **2006**, *6*, 170.

[21] A.E.W. Horst, S. Bormann, J. Meyer, M. Steinhagen, R. Ludwig, A. Drews, M. Ansorge-Schumacher, D. Holtmann, *J. Mol. Catal. B: Enzym.* **2016**.

[22] T. Krieg, S. Hüttmann, K.-M. Mangold, J. Schrader, D. Holtmann, *Green Chem.* **2011**, *13*, 2686.

[23] V. V. Kovačević, B. P. Dojčinović, M. Jović, G. M. Roglić, B. M. Obradović, M. M. Kuraica, *J. Phys. D: Appl. Phys.* **2017**, *50*, 155205.

[24] P. Rajasekaran, P. Mertmann, N. Bibinov, D. Wandke, W. Viöl, P. Awakowicz, *Plasma. Process. Polym.* **2010**, *7*, 665.

[25] Y. Wang, D. Lan, R. Durrani, F. Hollmann, *Curr. Opin. Chem. Biol.* **2017**, *37*, 1.

[26] N. C. Veitch, *Phytochemistry* **2004**, *65*, 249.

[27] G. I. Berglund, G. H. Carlsson, A. T. Smith, H. Szöke, A. Henriksen, J. Hajdu, *Nature* **2002**, *417*, 463.

[28] F. W. Krainer, A. Glieder, *Appl. Microbiol. Biotechnol.* **2015**, *99*, 1611.

[29] J.-W. Lackmann, S. Baldus, E. Steinborn, E. Edengeiser, F. Kogelheide, S. Langklotz, S. Schneider, L. I. O. Leichert, J. Benedikt, P. Awakowicz et al., *J. Phys. D: Appl. Phys.* **2015**, *48*, 494003.

[30] Z. Ke, Q. Huang, *Plasma. Process. Polym.* **2013**, *10*, 731.

[31] P. Attri, N. Kumar, J. H. Park, D. K. Yadav, S. Choi, H. S. Uhm, I. T. Kim, E. H. Choi, W. Lee, *Sci. Rep.* **2015**, *5*, 8221.

[32] J. de Backer, J. Razzokov, D. Hammerschmid, C. Mensch, Z. Hafideddine, N. Kumar, G. van Raemdonck, M. Yusupov, S. van Doorslaer, C. Johannessen et al., *Redox Biol.* **2018**.

[33] M. Kuchenbecker, N. Bibinov, A. Kaemlimg, D. Wandke, P. Awakowicz, W. Viöl, *J. Phys. D: Appl. Phys.* **2009**, *42*, 45212.

[34] M. Krewing, J. J. Stepanek, C. Cremers, J.-W. Lackmann, B. Schubert, A. Müller, P. Awakowicz, L. I. O. Leichert, U. Jakob, J. E. Bandow, *Journal of the Royal Society, Interface* **2019**, *16*, 20180966.

[35] M. Farasat, S. Arjmand, S. O. R. Siadat, Y. Sefidbakht, H. Ghomi, *Sci Rep*, *8*, 1.

[36] E. Nagababu, J. M. Rifkind, *Biochemistry* **2000**, *39*, 12503.

[37] E. Nagababu, J. M. Rifkind, *Antioxid. Redox. Signal.* **2004**, *6*, 967.

[38] J. J. P. Perry, D. S. Shin, E. D. Getzoff, J. A. Tainer, *Biochim. Biophys. Acta* **2010**, *1804*, 245.

[39] Y. Sheng, I. A. Abreu, D. E. Cabelli, M. J. Maroney, A.-F. Miller, M. Teixeira, J. S. Valentine, *Chem. Rev.* **2014**, *114*, 3854.

[40] T. Li, H. L. Bonkovsky, J.-t. Guo, *BMC Struct. Biol.* **2011**, *11*, 13.

[41] H. Zhang, Z. Xu, J. Shen, X. Li, L. Ding, J. Ma, Y. Lan, W. Xia, C. Cheng, Q. Sun et al., *Sci. Rep.* **2015**, *5*, 10031.

[42] S. Choi, P. Attri, I. Lee, J. Oh, J.-H. Yun, J. H. Park, E. H. Choi, W. Lee, *Sci. Rep.* **2017**, *7*, 1027.

[43] T. R. Brubaker, K. Ishikawa, K. Takeda, J.-S. Oh, H. Kondo, H. Hashizume, H. Tanaka, S. D. Knecht, S. G. Bilén, M. Hori, *J. Appl. Phys.* **2017**, *122*, 213301.

[44] M. Krewing, B. Schubert, J. E. Bandow, *Plasma Chemistry and Plasma Processing* **2019**.

[45] S. Goldstein, G. Czapski, *Int. J. Radiat. Biol. Relat. Stud. Phys. Chem. Med.* **1984**, *46*, 725.

[46] C. Klinkhammer, C. Verlackt, D. śmiłowicz, F. Kogelheide, A. Bogaerts, N. Metzler-Nolte, K. Stapelmann, M. Havenith, J.-W. Lackmann, *Sci. Rep.* **2017**, *7*, 13828.

[47] S. K. Pankaj, N. N. Misra, P. J. Cullen, *Innov. Food Sci. Emerg. Technol.* **2013**, *19*, 153.

[48] I. Bekard, D. E. Dunstan, *Soft Matter* **2014**, *10*, 431.

[49] K. Stapelmann, J.-W. Lackmann, I. Buerger, J. E. Bandow, P. Awakowicz, *J. Phys. D: Appl. Phys.* **2014**, *47*, 85402.

[50] P. J. Bruggeman, M. J. Kushner, B. R. Locke, J. G. E. Gardeniers, W. G. Graham, D. B. Graves, R. C. H. M. Hofman-Caris, D. Maric, J. P. Reid, E. Ceriani et al., *Plasma Sources Sci. Technol.* **2016**, *25*, 53002.

[51] M. Okuda, T. Tsuruta, K. Katayama, *Phys. Chem. Chem. Phys.* **2009**, *11*, 2287.

[52] X. Lu, G. V. Naidis, M. Laroussi, S. Reuter, D. B. Graves, K. Ostrikov, *Phys. Rep.* **2016**, *630*, 1.

[53] P. Attri, Y. H. Kim, D. H. Park, J. H. Park, Y. J. Hong, H. S. Uhm, K.-N. Kim, A. Fridman, E. H. Choi, *Sci. Rep.* **2015**, *5*, 9332.

[54] F.-J. Schmitt, G. Renger, T. Friedrich, V. D. Kreslavski, S. K. Zharmukhamedov, D. A. Los, V. V. Kuznetsov, S. I. Allakhverdiev, *Biochim. Biophys. Acta* **2014**, *1837*, 835.

[55] W. Zhang, E. Fernández-Fueyo, Y. Ni, M. van Schie, J. Gacs, R. Renirie, R. Wever, F. G. Mutti, D. Rother, M. Alcalde et al., *Nat. Catal.* **2018**, *1*, 55.

[56] M. Kluge, R. Ullrich, K. Scheibner, M. Hofrichter, *Green Chem.* **2012**, *14*, 440.

[57] M. J. Pecyna, R. Ullrich, B. Bittner, A. Clemens, K. Scheibner, R. Schubert, M. Hofrichter, *Appl. Microbiol. Biotechnol.* **2009**, *84*, 885.

[58] P. Molina-Espeja, E. Garcia-Ruiz, D. Gonzalez-Perez, R. Ullrich, M. Hofrichter, M. Alcalde, *Appl. Environ. Microbiol.* **2014**, *80*, 3496.

[59] J. L. Lepe-Zuniga, J. S. Zigler, I. Gery, *J. Immunol. Methods.* **1987**, *103*, 145.

[60] M. Kirsch, E. E. Lomonosova, H.-G. Korth, R. Sustmann, H. Groot, *J. Biol. Chem.* **1998**, *273*, 12716.

[61] P. Molina-Espeja, S. Ma, D. M. Mate, R. Ludwig, M. Alcalde, *Enzyme and Microbial Technology* **2015**, *73-74*, 29.

[62] P. C. F. Graf, M. Martinez-Yamout, S. VanHaerents, H. Lilie, H. J. Dyson, U. Jakob, *J. Biol. Chem.* **2004**, *279*, 20529.